
ELSEVIER
Review of
Palaeobotany
& Palynology

Review of Palaeobotany and Palynology 189 (2013) 8–17

Contents lists available at SciVerse ScienceDirect

Review of Palaeobotany and Palynology

journal homepage: www.elsevier.com/locate/revpalbo

Research paper

Climate instability during the last deglaciation in central Asia, reconstructed by pollen data from Yili Valley, NW China

Keliang Zhao [a,b], Xiaoqiang Li [a,b,*], John Dodson [c], Xinying Zhou [a,b], Pia Atahan [c]

[a] The Laboratory of Human Evolution, Institute of Vertebrate Paleontology and Paleoanthropology, Chinese Academy of Sciences, 142 Xizhimenwai Street, Beijing 100044, China
[b] State Key Laboratory of Loess and Quaternary Geology, Institute of Earth Environment, Chinese Academy of Sciences, Xi'an 710075, China
[c] Institute for Environmental Research, Australian Nuclear Science and Technology Organisation, Kirrawee, NSW 2232, Australia

ARTICLE INFO

Article history:
Received 15 May 2012
Received in revised form 11 October 2012
Accepted 23 October 2012
Available online xxxx

Keywords:
Yili Valley
central Asia
late MIS3
last deglaciation
Bølling–Allerød warm period
Younger Dryas

ABSTRACT

An extended pollen record with grain size analysis and AMS ^{14}C dating is provided for a palaeolake section which is located in an intermountain basin in Yili Valley, Xinjiang, NW China. Covering the late MIS 3, early MIS 2 and the last deglaciation, vegetation variations and climate events are discussed in relation to changes in pollen assemblages and *Artemisia*/Chenopodiaceae (A/C) ratios. The presence of montane forest-steppe dominated by *Picea* and *Taraxacum* indicates a relative humid climate in the study area during late MIS 3 (before 31.5 cal kyr BP). *Picea* forest disappeared and the vegetation dominated by Chenopodiaceae shows the climate became dry from 31.5 to 14.7 cal kyr BP. The sediments of Last Glacial Maximum (LGM) period are absent in the section probably. *Betula-Picea* mixed forest occurred at 14.7 cal kyr BP and corresponds to the onset of the warm Bølling period in the North Atlantic. A long dry period was detected from 14.5 to 13.6 cal kyr BP on the basis of the occurrence of Chenopodiaceae desert. A subalpine meadow community dominated by *Geranium* covered the area during 13.6–13.4 cal kyr BP, suggesting lower temperatures at this time. This may coincide with the Older Dryas (OD). The most humid period in the record occurred between 13.4 and 12.9 cal kyr BP, which coincides with the warm Allerød period. Dry conditions prevailed from ~12.9 to 11.7 cal kyr BP in the area, coinciding with the Younger Dryas (YD) in the North Atlantic. Within this period a three-phase climate fluctuation was detected, which can be summarized as follows: a dry early YD (12.9–12.6 cal kyr BP), a slightly moister mid-YD (12.6–12.0 cal kyr BP) and a very dry late YD (12.0–11.7 cal kyr BP). These millennial to century-scale climatic events in Yili Valley correlate well with other palaeoclimate records in North Hemisphere, suggesting that these events probably originate from same mechanisms.

1. Introduction

The last deglaciation represents the transition from the Last Glacial Maximum (LGM) to the postglacial epoch (Holocene). It was a period characterized by rising global temperatures, rapid collapse of ice sheets and a large rise in sea level (Ruddiman and McIntyre, 1981; Blanchon and Shaw, 1995; Sowers and Bender, 1995). Understanding the sequence of climatic events surrounding the last deglaciation is essential for understanding dynamics of the earth's surface systems (Yu and Wright, 2001; Barker et al., 2009), and for accurately evaluating future climate trends under global warming (Parizek and Alley, 2004; Liu et al., 2009).

In a general sense, climate systems can be described as moving from one stable state to another over time (Stocker and Wright, 1991; Blunier and Brook, 2001). This process can be illustrated by the millennial to century-scale climatic events that occurred in the Northern Hemisphere during the last deglaciation, such as the Bølling–Allerød (BA), Older Dryas (OD), Younger Dryas (YD) and Preboreal events which are clearly evident in isotopic records from Greenland ice cores, North Atlantic marine sediments and European and North American lake sediments (Dansgaard et al., 1989; Lehman and Keigwin, 1992; Lotter et al., 1992; Alley et al., 1993; Yu and Eicher, 1998). Rapid climate oscillations such as these provide a good opportunity to study mechanisms associated with the Earth's climate systems.

Due to recent improvements in the resolution and dating precision of palaeoclimate work in monsoonal Asia, important information about the rate, amplitude and driving mechanisms of climate events during the last deglaciation is now available (Porter and An, 1995; Sirocko et al., 1996; Nakagawa et al., 2006). Oxygen isotope records of stalagmites from Dongge and Hulu Cave suggested that oscillations of the Asian monsoon were rapid and synchronous with Greenland temperatures during the last deglaciation (Wang et al., 2001; Yuan et al., 2004). The same signals of rapid climate oscillations have been detected in the sediment records of Qinghai and Huguangyan Maar lake (Shen et al., 2005; Yancheva et al., 2007).

* Corresponding author at: The Laboratory of Human Evolution, Institute of Vertebrate Paleontology and Paleoanthropology, Chinese Academy of Sciences, 142 Xizhimenwai Street, Beijing 100044, China.
E-mail address: lixiaoqiang@ivpp.ac.cn (X. Li).

0034-6667/$ – see front matter © 2012 Elsevier B.V. All rights reserved.
http://dx.doi.org/10.1016/j.revpalbo.2012.10.005

Despite the large number of climate reconstructions covering the last deglaciation in the central Asia using lake sediments, where the mid-latitude westerlies are a dominant climatic influence (Fig. 1), there is considerable disagreement over past climatic characteristics of the region. River inflow to the Caspian Sea rose sharply during the warmer BA and fell equally sharply during the YD (Thom, 2010). The variations in $\delta^{13}C$ and $\delta^{18}O$ from Baikal Lake closely align with Northern Hemisphere temperatures during last deglaciation, and clearly reflect the BA and YD climatic events (Prokopenko and Williams, 2004; Morley et al., 2005). A sediment record from Hovsgol Lake, northwest Mongolia, indicates the water volume gradually increased during the last deglaciation, but does not show abrupt climate shifts such as the BA and YD events (Murakami et al., 2010). A major filling episode for the Aral Sea occurred between the late Pleistocene and early Holocene (Boomer et al., 2000), while records from sites such as Bosten and Barkol Lakes show dry conditions during the last deglaciation (Huang et al., 2009; Tao et al., 2010). Existing evidence shows a complicated picture of climate changes in central Asia during the last deglaciation, and more work using robust dating techniques and high resolution records are needed for the region.

Located in central Asia, far from oceanic influences, the climate of the Yili Valley is chiefly influenced by the mid-latitude westerlies (Li, 1991). This makes it an ideal site for assessing climate variations in central Asia. This study utilizes a 1220 cm long sediment section collected in 2009 from the Yili Valley. The sediment section is believed to have been deposited under lacustrine conditions. Vegetation and climate variations are reconstructed during the last deglaciation in the study region, using AMS^{14}C dating, grain size analysis and a high resolution pollen record. This work builds on earlier work at the site by Li et al. (2011), which focused on the upper 900 cm of the sediment section. The timing and characteristics of climate events in the Yili Valley are determined, and used to discuss climatic forcing mechanisms for this and other regions in the Northern Hemisphere during the deglaciation.

2. Study area

The Yili Valley is located in the Tian Shan Mountain range of central Asia. Mountain slopes border the valley to the north, south and east (Fig. 1). The Yili Valley has a temperate semi-arid continental climate. Westerly winds prevail throughout the year. During winter the climate is controlled mostly by the intensity and position of the Siberian high pressure cell, and is mainly influenced by the northern stream of the westerly airflow. During summer the mid-latitude westerlies shift northwards and the southern stream of the airstream affects the Yili valley (Li, 1991). The Yili Valley is in a relatively high precipitation zone of Xinjiang Province, as a result of its exposure to humid and warm airflow from the west. Topography has a large influence on the mean annual temperature (MAT) and mean annual precipitation (MAP) of the region. MAT ranges from 2.6 to 10.4 °C, while MAP is between 200 and 500 mm on the valley plains and up to 800 mm in mountain zones.

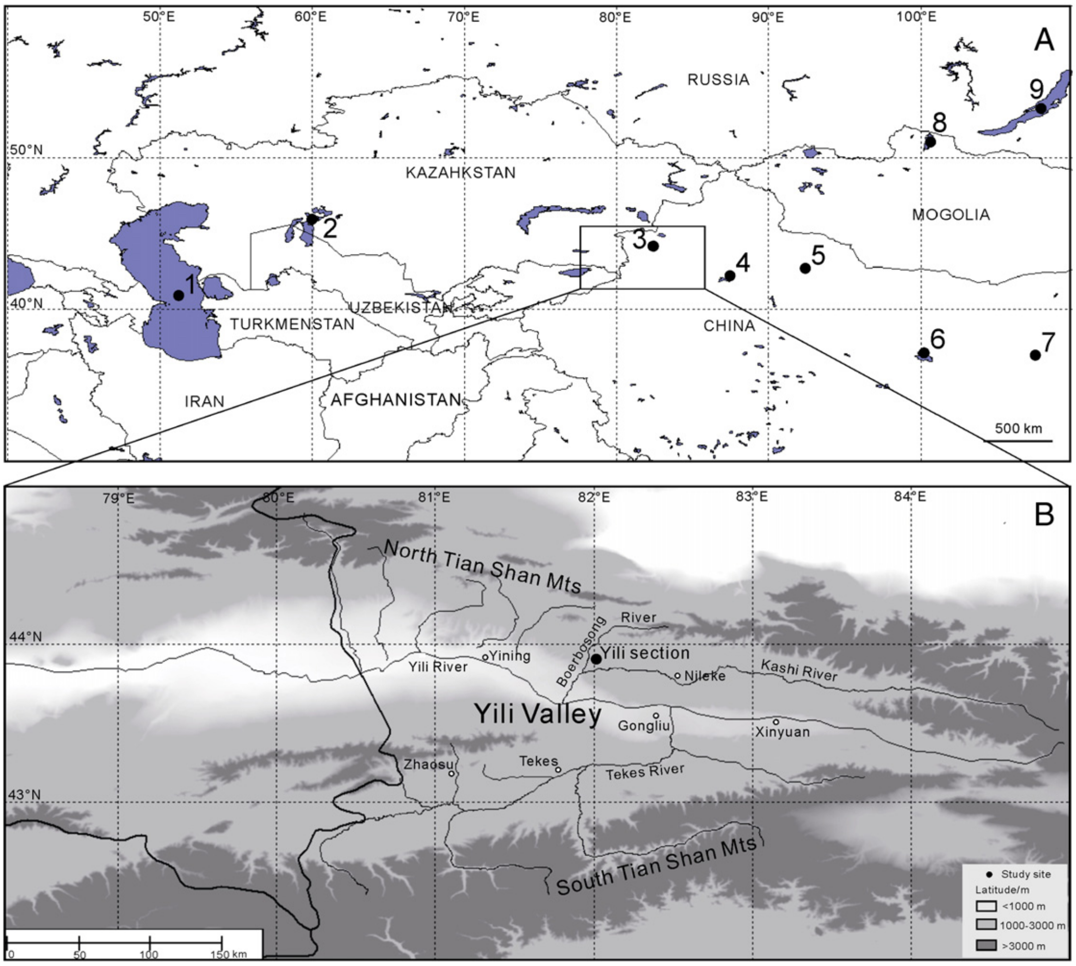

Fig. 1. The study site and other sites referred to in the text in central Asia (A) and the position of Yili section in Yili Valley (B): 1, Caspian Sea (Thom, 2010); 2, Aral Sea (Boomer et al., 2000); 3, Yili section (this study); 4, Bosten Lake (Huang et al., 2009); 5, Barkol Lake (Tao et al., 2010); 6, Qinghai Lake (Shen et al., 2005); 7, Midiwan section (Li et al., 2003); 8, Hovsgol Lake (Murakami et al., 2010); and 9 Baikal Lake (Prokopenko and Williams, 2004).

Vegetation zones of the Yili valley are vertically distributed and are classified in descending order as: alpine cushion-like vegetation; alpine meadow; subalpine meadow; montane forest–meadow; montane steppe and desert (Fig. 2) (Xinjiang Expedition Team, 1978). The cushion-like vegetation zone occurs above ~3000 m a.s.l. and is dominated by *Sibbaldianthe tetrandra* and *Thylacospermum caespitosum*. The alpine meadow zone occurs between ~2800 and 3200 m a.s.l. and is composed of *Cobresia capilliforms*, *Carex stenocarpa*, *C. cobressiformis* and *Polygonum viviparum*. The subalpine meadow zone occurs from ~2400–2700 m a.s.l. and is dominated by *Alchemilla obtuse*, *Geranium albiflorum*, *Geranium collinum*, *Phlomis oreophila*, *Thalictrum alpinum*, *Gentiana tianschenica*, *Poa annua* and *Brachypodium pinnatum*. The montane forest–meadow zone occurs between ~1500 and 2800 m a.s.l. and consists of *Picea* forest and steppe or meadow. Patches of *Picea* forest occur on shady and wet mountain slopes. The montane steppe zone occurs on the piedmont between ~1000 and 1600 m a.s.l. and consists predominantly of *Stipa capillata*, *Festuca rupicola*, *Bothriochloa ischaemun*, *Caragana turkestanica* and *Rosaerea* sp. The desert zone occurs below ~1100 m a.s.l. and is dominated by *Artemisia boratalensis*, *Artemisia kaschgaria*, *Kochia prastrata*, *Poa bulbosa*, and *Alyssum desertorum* (Xinjiang Expedition Team, 1978) (Fig. 2).

3. Study materials and methods

3.1. Sediment and dating

The Yili section (43°51′25.7″N, 81°57′54.3″E; 928 m a.s.l.) is located in an intramountain basin in Maza town, Yili city, Xinjiang Province. The section is 1220 cm deep and the upper 900 cm of the section has previously been described by Li et al. (2011). The sediments are composed of silts, sands and clays, a description of the lithology is provided in Fig. 3. A total of 244 sediment samples were collected at 5 cm intervals through the section. Eight charcoal samples and three shell samples were selected for AMS^{14}C dating. Sample pretreatment and measurement was carried out at the Australian Nuclear Science and Technology Organization, Australia. Radiocarbon dates have been converted to calibrated ages according to Reimer et al. (2009) (Table 1).

The linear interpolation method used to model ages between the depths of 890 cm and 125 cm is described by Li et al. (2011). AMS^{14}C dating was not conducted above 125 cm, as the section above this had signs of modern disturbance from agricultural activity. An AMS^{14}C date on a shell collected at 958–960 cm depth reveals a period of very slow sedimentation or a hiatus, during the LGM (Fig. 3). Radiocarbon dates are absent in the lowest 260 cm of the section, and as a result the basal age of the Yili section is uncertain.

Grain size increases abruptly at 890 cm, indicating that meltwater brought coarser sediment at the beginning of last deglaciation (Fig. 3). Based on the variations of grain sizes and the time span between 960 and 890 cm (70 cm thicker covering ~17000 yr), we conclude that a sedimentary lacuna from 960 to 890 cm is possible. Potential reasons for this are: 1) the lake shrank considerably or even dried up during LGM, resulting in exposure and erosion; and 2) a strong hydrodynamic force at the beginning of deglaciation denuded part of the original sediment at the site. According to the analysis above, we suggest that the depth of 1220–890 cm corresponds to the late MIS 3 to early MIS 2, and that the sediments of the LGM period were lost (Fig. 3).

3.2. Pollen analysis methods

A total of 78 samples were prepared for pollen analysis between 400 and 1220 cm depth, covering the time period from MIS 3 to the last deglaciation. Results for the 52 pollen samples between 400 and 900 cm depth have been discussed by Li et al. (2011). Pollen samples were prepared from 150 g of sediment using heavy liquid separation (Moore and Webb, 1978; Li and Du, 1999) and acetolysis (Erdtman, 1960). *Lycopodium* tablets were added to the samples to allow for estimation of pollen concentrations. About 40,000 pollen grains were identified in all 78 samples. At least 300 pollen grains were counted for most of the samples. Low pollen abundance resulted in pollen counts of less than 300 grains in 9 samples. Pollen morphological keys were used to identify pollen taxa (e.g. Xi and Ning, 1994; Wang et al., 1997). *Artemisia*, *Aster*-type and *Taraxacum*-type pollen grains were counted separately to other Compositae grains. Pollen percentages are calculated from the sum of the arboreal and non-arboreal taxa identified in each pollen spectrum (Fig. 4).

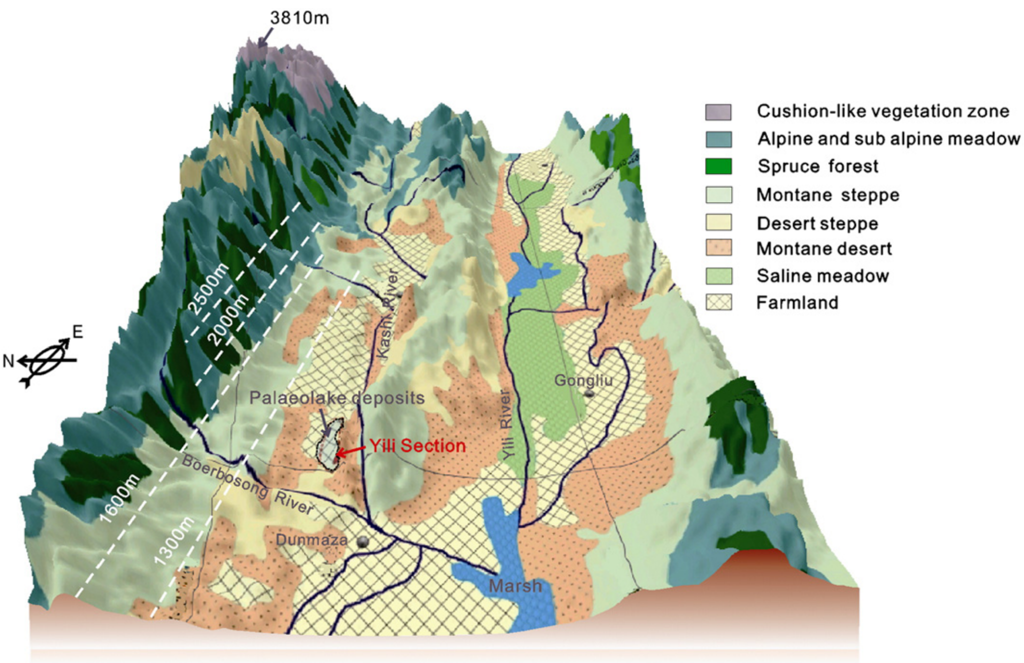

Fig. 2. Vertical vegetation zones around the study site in the Yili Valley.

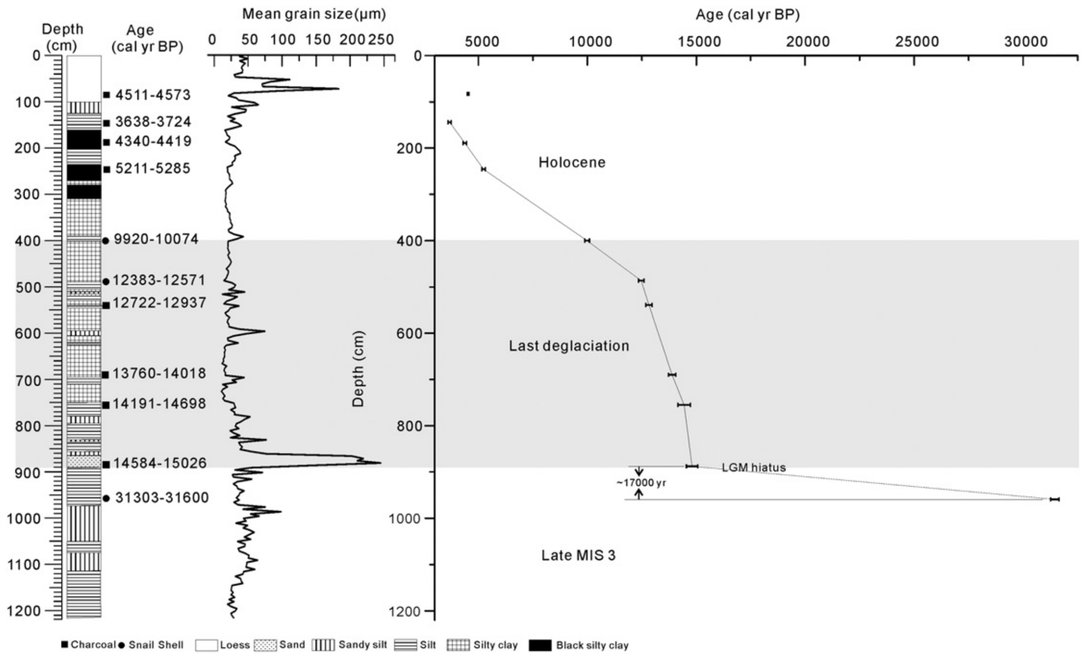

Fig. 3. The age-depth model in Yili section. The section of last deglaciation was marked by light-gray shadow. Full lines show the results of interpolation, and dotted line represents deposit hiatus between two points.

3.3. Interpretation methods

Previous publications are drawn on for the interpretation of the Yili section pollen data, particularly those dealing with characteristic surface pollen assemblages for the region and indicator taxa (Xinjiang Expedition Team, 1978; Editorial Committee for Vegetation of China, 1980; Yan, 1991, 1993; Weng et al., 1993; Xu et al., 1996; Cour et al., 1999; Luo et al., 2009). Modern pollen studies from surface lake sediment show that the pollen records in the lake sediment are indicative of nearby vegetation and pollen grains were transported to the palaeolake by wind and surface flow (e.g. Herzschuh et al., 2006a; Shang et al., 2009; Zhao and Herzschuh, 2009).

Artemisia and Chenopodiaceae are dominant taxa in arid areas of central Asia and the ratio of pollen of those taxa can be used as an indicator of moisture level. In desert regions, Chenopodiaceae pollen tends to be higher than *Artemisia*, while in steppe-like wetter environments, *Artemisia* pollen dominates. EL-Moslimany (1990) demonstrated the usefulness of the *Artemisia*/Chenopodiaceae (A/C) ratio by studying modern pollen spectra in the Middle East. Later work found the A/C ratio to also be a good indicator of effective moisture in parts of northwest China, such as the West Kunlun Mountains (Weng et al., 1993), southeastern Inner Mongolia (Liu et al., 1999), the Alashan Plateau (Herzschuh et al., 2004), northwestern Tibet (Huang et al., 1993; Cour et al., 1999), and the Xinjiang region (Luo et al., 2009). The A/C ratio has now been widely applied in palaeoclimate studies in arid regions of Asia (Gasse et al., 1991; Herzschuh et al., 2006b; Chen et al., 2008). The sum of *Artemisia* and Chenopodiaceae pollen in the Yili section averages 60.9% of the total pollen counts, and this is considered to be sufficiently high for the ratio to be used as an indicator of moisture levels (Sun et al., 1994).

Table 1
AMS^{14}C dating results from the Yili section.

Lab code	Depth (cm)	Sample type	^{14}C ages (yr BP)	Calibrated ages (cal yr BP)
OZL450	82–84	Charcoal	4050 ± 35	4511–4573
OZL451	143–145	Charcoal	3440 ± 40	3638–3724
OZL452	188–190	Charcoal	3915 ± 40	4340–4419
OZL453	245–247	Charcoal	4490 ± 50	5211–5285
OZL476	400	Shell	8910 ± 60	9920–10,074
OZL487	486–487	Shell	10,500 ± 70	12,383–12,571
OZL456	538–540	Charcoal	10,980 ± 60	12,722–12,937
OZL290	690	Charcoal	12,030 ± 120	13,760–14,018
OZL457	755	Charcoal	12,430 ± 70	14,191–14,698
OZM456	885–890	Charcoal	12,560 ± 60	14,584–15,026
OZL478	958–960	Shell	27,330 ± 200	31,303–31,600

Compositae is distributed widely in Xinjiang (Xinjiang Expedition Team). Although the relationship between the percentage of Compositae pollen and its representation in the vegetation cover of the region is not clear, pollen of Compositae (excluding *Artemisia* species) is abundant in alpine and subalpine meadows of Xinjiang (Luo et al., 2009). *Aster*-type pollen occurs mainly in mountain environments; and *Taraxacum*-type pollen can be used as an indicator of humid conditions (Ma et al., 2009). *Geranium* and *Alchemilla* are the dominant plants of subalpine meadows, which lie above the montane forest–meadow and montane steppe zones of the Yili Valley (Xinjiang Expedition, 1978).

Modern pollen studies show that *Betula* pollen is abundant in coniferous–broad-leaved mixed forests on the Alatai and Tian Shan Mountains. There, *Betula* pollen usually comprises around 5–10% of the total pollen sum for surface samples and can reach 20–30% (Luo et al., 2009). In the Yili section, *Betula* pollen accounts for as much as 25% of the total pollen sum in some samples and this must result from the growth of *Betula* at the study site.

Surface pollen studies show that *Picea* pollen abundance is closely related to the plant's coverage (Xu et al., 2007), *Picea* pollen is reported to account for more than 5% of pollen in the surface soil of areas where *Picea* occurs (Yan et al., 2004). In the Yili section, *Picea* pollen percentages reach 22.2%, indicating the occurrence of *Picea* forest at the study site.

4. Results

A total of 43 pollen types were identified in the Yili section. Pollen spectra are dominated by non-arboreal pollen (NAP), which constitutes

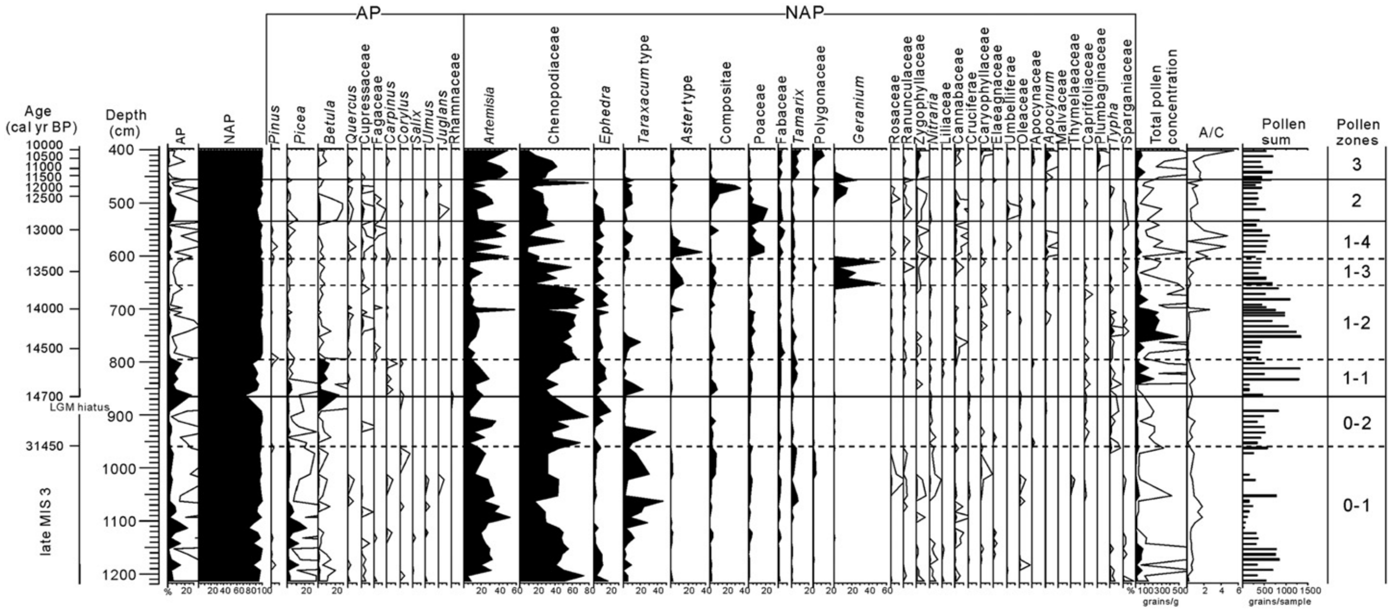

Fig. 4. Pollen percentages diagram of Yili section. 10 × exaggeration for the less abundant taxa, AP and the total pollen concentration.

on average 96.7% of the total pollen sum. Chenopodiaceae and *Artemisia* are the main components of NAP. Those taxa contribute on average 60.9% of the total pollen sum. Arboreal pollen (AP) is dominated by *Betula* and *Picea*, contributing up to 24.8% and 22.2% of total pollen sum.

Four pollen zones have been identified in the Yili section, between the depths of 1220 and 400 cm. These zones are based on differences in pollen assemblages and A/C ratios (Fig. 4).

4.1. PZ 0 (1220–865 cm, late MIS 3 to 14.7 cal kyr BP)

This zone is characterized by high proportions of Chenopodiaceae, *Artemisia* and *Taraxacum*-type, and variable proportions of AP. This zone has been divided into two sub-zones.

4.1.1. PZ 0–1 (1220–960 cm, late MIS3)

Chenopodiaceae contents contribute on average 42.1% of the total pollen sum in this sub-zone. *Artemisia* and *Taraxacum*-type pollens account for 25.8% and 11.2% respectively. AP percentages are also high in this sub-zone. *Picea* composes on average 5% of the total pollen sum and has a maximum of 22.2%. The pollen assemblages indicate that the *Picea* forest–montane steppe occurred in the vicinity of the study site. The A/C values reach 1.8 in this sub-zone and have an average of 0.7. Overall, the pollen assemblage and A/C ratios point to a relatively humid climate for this sub-zone.

4.1.2. PZ 0–2 (960–865 cm, 31.5 to 14.7 cal kyr BP)

The average Chenopodiaceae pollen percentage for sub-zone PZ 0–2 rises to 54.9%, and has a maximum of 79.2%. *Artemisia* pollen falls to an average of 17.5% of the total pollen sum. *Picea* pollen percentages are markedly lower than sub-zone PZ 0–1 (1.4% average), indicating the disappearance of *Picea* forest from the site. A/C ratios are low (0.4 average), indicating that the climate was drier than PZ 0–1.

4.2. PZ 1 (865–545 cm, 14.7–12.9 cal kyr BP)

PZ 1 is dominated by the NAP. AP pollen is high below 795 cm depth, but decreases gradually towards the top of the zone. Pollen concentrations are higher than the underlying zone (PZ0). A/C ratios range from 0.1 to 4.7. This zone has been divided into four sub-zones.

4.2.1. PZ 1-1 (865–795 cm, 14.7–14.5 cal kyr BP)

The main feature of this sub-zone is the marked rise in *Betula* pollen at the commencement of the sub-zone. *Picea* pollen also rises, but to a lesser degree. *Betula* pollen averages 10.3% of the total pollen sum and has a maximum of 24.8%, while *Picea* reaches 4.5% of the total pollen sum. This indicates that a coniferous–broad-leaved mixed forest occurred around the site at this time. Chenopodiaceae percentages decline (average 37.8%) while the *Artemisia* percentages increase slightly (19% average). The A/C ratios range from 0.1 to 1.0 and have an average of 0.5, pointing to a wetter climate in comparison to PZ 0–2.

4.2.2. PZ 1–2 (795–655 cm, 14.5–13.6 cal kyr BP)

This sub-zone is dominated by Chenopodiaceae pollen, which reaches 59.1% of the total pollen sum. *Artimisia* contents decline in comparison to the previous zone. *Betula* pollen is substantially less abundant than sub-zone PZ 1–1, maximizing at 1.6%. A/C ratios are mostly low throughout this sub-zone (0.3 average). An isolated peak of 2.6 at 700–705 cm depth (ca. 14 cal kyr BP) suggests a temporary increase in moisture levels. Overall the pollen assemblages and the A/C ratios indicate desert vegetation communities dominated by Chenopodiaceae, and suggest a dry climate.

4.2.3. PZ 1–3 (655–605 cm, 13.6–13.4 cal kyr BP)

This sub-zone is characterized by markedly high percentages of *Geranium* pollen (29.6% average with a maximum of 52.7%), coinciding with low percentages of Chenopodiaceae, *Artemisia* and *Ephedra*. A small increase in *Aster*-type and Compositae pollen also characterizes this sub-zone. A/C ratios have an average of 0.4, implying an increase of moisture in comparison to PZ 1–2. Overall the pollen assemblages show a subalpine meadow vegetation community dominating the study area during this period.

4.2.4. PZ 1–4 (605–535 cm, 13.4–12.9 cal kyr BP)

Sub-zone PZ 1–4 is characterized by increased percentages of *Artemisia* pollen (34.2% average), Poaceae (8.9% average), *Aster*-type (4.7% average) and *Taraxacum*-type (8.9% average). Chenopodiaceae percentages are at their lowest in this sub-zone, composing on average 22.5% of the total pollen sum. A/C ratios range from 0.1 to 4.7 and have an average of 2.3. Overall the pollen assemblages and A/C ratios show steppe vegetation communities prevailing in the study area, with a warmer and more humid climate.

4.3. PZ 2 (535–455 cm, 12.9–11.7 cal kyr BP)

Pollen spectra for this pollen zone are dominated by Chenopodiaceae (29.5% average), *Artemisia* (20.4% average), Compositae (11.5% average), *Geranium* (7.7% average), *Taraxacum*-type (6.8% average) and Poaceae (6.4% average). The A/C ratios range from 0.1 to 1.8 and have an average of 0.9. The pollen assemblages and the A/C ratios point to a subalpine meadow community with a cold and relative dry climate during this period. Chenopodiaceae peaks at 79% at 460–465 cm depth (~11.8 cal kyr BP), which corresponds with an A/C ratio of 0.1, indicating the presence of desert vegetation communities. This is the most arid period detected during the last deglaciation of the Yili section.

4.4. PZ 3 (455–400 cm, 11.7–10.1 cal kyr BP)

The commencement of zone PZ 3 is marked by an increase in *Artemisia* pollen, which remains high through the zone (41.0% average). Chenopodiaceae percentages are lower than the underlying zone (27.7% average), while Fabaceae, Polygonaceae and *Tamarix* percentages are higher. A/C ratios range from 0.7 to 5.5 and have an average of 2.0. Overall the pollen and A/C data indicate the dominance of shrub steppe vegetation communities and the amelioration of climate conditions.

5. Discussion and conclusions

A lack of radiocarbon dates below 960 cm results in the age estimation for the lower part of the Yili section being tenuous. Given that the radiocarbon age at 958–960 cm depth is 31,303–31,600 cal yr BP, the lowest pollen subzone (PZ 0–1; 1220–960 cm depth) predates 30,000 yr BP, placing it in the late MIS 3. During this time palaeoclimate records from ice cores and lake sediments suggest an exceptionally warm and humid climate in the Tibetan Plateau (Shi et al., 2001) and warmer conditions globally (Imbrie et al., 1984). During the late MIS 3 forests expanded in the Luanhaizi Lake area and temperatures were slightly above present-day levels in the Qilian Mountains (Herzschuh et al., 2006a). Both the presence of montane forest-steppe and higher A/C ratios in the Yili record point to a humid climate in the study area during PZ 0–1, which possibly corresponds to the late MIS 3.

A drier climate during PZ 0–2 (960–865 cm) is suggested by the disappearance of *Picea* forest from the site and a decrease in A/C ratios. This period possibly corresponds to the transition between the warm and wet late MIS 3 to the cold-dry MIS 2. Similarly dry conditions can be found in other regions of central Asia. At Baikal Lake, sedimentary organic matter declines across the MIS 3/MIS 2 transition (Swann et al., 2005), and in monsoonal central Asia, moisture levels are lower during MIS 2 (Herzschuh, 2006).

The section from 960 to 865 cm covers the LGM period and probably includes a sedimentary hiatus, due either to a break in sedimentation or erosion. The hiatus suggests a dry climate prevailed in the Yili Valley during the LGM. At this time sparse alpine vegetation and alpine deserts occurred in the vicinity of Luanhaizi Lake, indicating dry conditions in the Qilian Mountains (Herzschuh et al., 2006a). Very low water levels are reported at Hovsgol Lake in Mongolia during the LGM (Prokopenko et al., 2005), and at Baikal and Hovsgol lakes planktonic and benthic diatoms are absent in the sedimentary records (Karabanov et al., 2004). Other studies in western China, however, argue for higher lake levels at the LGM due to lower evaporation (Yu et al., 2003). Further palaeoecological work in areas such as Xinjiang is needed to understand conditions during the LGM in central Asia.

The last deglaciation is represented in the Yili section between the depths of 865–400 cm. Six AMS^{14}C dates between those depths indicate that these sediments were deposited between about 14.7 and 10.1 cal kyr BP, and individual pollen samples between these depths represent between about 50–100 years of deposition. Vegetation and climate variations in the Yili Valley during this deglaciation are discussed below and compared with other records from the Northern Hemisphere.

Palaeoclimate records from Greenland, the North Atlantic, Europe, North America and Asia indicate that during the last deglaciation the climate was unstable and included a series of millennial to century-scale climate events (Lehman and Keigwin, 1992; Dansgaard et al., 1993; Hughen et al., 1996; Benson et al., 1997; Von Grafenstein et al., 1999; Rasmussen et al., 2006). The warm BA period (~14.7–12.9 cal kyr BP) was punctuated by several century-scale cold events, including the intra-Bølling cold period (IBCP), Older Dryas (OD) and intra-Allerød cold period (IACP) (Fig. 5). The cold YD climate reversal occurred after the BA, and the climate entered into the warm Preboreal at ~11.7 cal kyr BP (Alley et al., 1993; Rasmussen et al., 2006) (Fig. 5). Evidence of these climate events can also be found in parts of arid and semi-arid Asia. Warmer and wetter conditions in the Qinghai Lake region around 15.4–14.1 cal kyr BP and 13.7–12.9 cal kyr BP possibly correlate with the Bølling and Allerød warming, while cold and dry events occurring around 14.1–13.7 cal kyr BP and 12.9–12.1 cal kyr BP appear to correlate with the OD and YD events respectively (Shen et al., 2005). Rising water levels ca. 15.4 cal kyr BP at Hovsgol Lake, northwest Mongolia, are probably a result of higher precipitation caused by the warmer climate (Prokopenko et al., 2005). However at Bosten Lake, palaeoclimate evidence shows a dry regional climate around 16–8 cal kyr BP (Huang et al., 2009).

The appearance of a *Picea-Betula* mixed forest in the Yili Valley around 14.7 cal kyr BP, as shown by the marked rise of *Betula* and *Picea* pollen, indicates that the climate was warmer and wetter than previously (Figs. 4, 5). The warm Bølling period began ~14.69 ± 0.18 kyr BP in Greenland, based on the GICC05 time scale provided by Rasmussen et al. (2006). Sea surface temperatures (SSTs) in the mid-latitudes of the western North Atlantic increased rapidly to 15–17 °C at ~15 kyr BP (Rodrigues et al., 2010). Also, the stalagmite record from Hulu Cave shows the Asia monsoon to have strengthened around 14,645 ± 60 yr BP, corresponding closely to the onset of the warm Bølling period in the North Atlantic (Wang et al., 2001). The timing of warmer and wetter conditions in the Yili Valley during the last deglaciation is synchronous with the onset of the warm Bølling period in Greenland, the North Atlantic and monsoonal Asia, which is attributed to increased summer insolation in the Northern Hemisphere (Berger and Loutre, 1991) (Fig. 5).

Increased aridity in the Yili Valley around 14.5 to 13.6 cal kyr BP is indicated by the dominance of Chenopodiaceae and desert vegetation communities, the disappearance of mixed forest from the area and lower A/C ratios. This dry period in the Yili valley coincides with the Melt Walter Pulse 1A event, which is reported to have occurred ~14.2–13.7 cal kyr BP (Clark and Mix, 2002). A brief return to wetter conditions ~14.0 cal kyr BP is indicated by high A/C values, which increase to 2.6.

An expansion of the subalpine vegetation zone in the study region is detected around 13.6–13.4 cal kyr BP, based on increased proportions of *Geranium* pollen in the Yili section. This vegetation change suggests cooler conditions at this time, and this may correspond with the OD event (Fig. 5).

The Yili pollen record indicates that between 13.4 and 12.9 cal yr BP montane steppe vegetation occurred in the area, and was dominated by Poaceae, *Aster*-type and *Artemisia*. The average A/C ratio was 2.3. This period appears to have been the most humid in the Yili Valley during the last deglaciation, and it coincides with the warm Allerød period. A low A/C ratio around 13.1 cal kyr BP (570–575 cm depth) suggests a short-lived period of dry conditions, and this dry period happens to coincide with the IACP in the North Atlantic, which occurred during the Allerød period (Fig. 5). Overall, moisture levels in the Yili Valley appear to have oscillated during the warm BA period, however underlying those oscillations is a rising trend that corresponds to increasing SSTs in the North Atlantic (Bard et al., 2000).

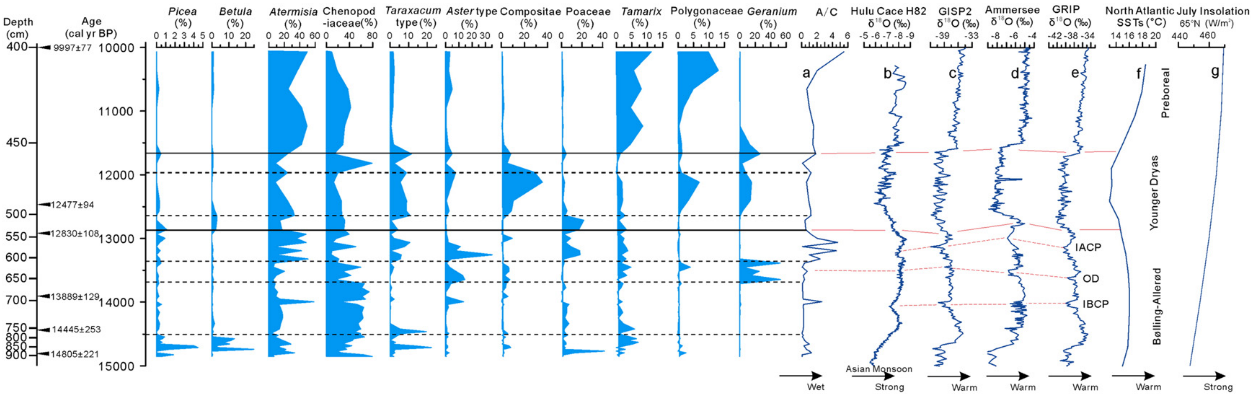

Fig. 5. Comparison between changes of main pollen assemblages and moisture in Yili Valley and selected records in North Hemisphere during the last deglaciation. (a) A/C in Yili Vally (this study); (b) $\delta^{18}O$ of stalagmite in Hulu Cave H82 (Wang et al., 2001); (c) $\delta^{18}O$ of ice-core GISP2 (Stuiver et al., 1995); (d) $\delta^{18}O$ of lacustrine carbonates at Ammersee Lake in Europe (Von Grafenstein et al., 1999); (e) $\delta^{18}O$ of ice-core GISP (Rasmussen et al., 2006); (f) SSTs of the North Atlantic (Bard et al., 2000); and (g) Northern Hemisphere July Insolation at 65°N (Berger and Loutre, 1991).

Table 2
Results of vegetation and climate reconstruction from Yili section pollen record.

Pollen zones	Depth (cm)	Age (cal kyr BP)	Characteristic pollen taxa	Vegetation construction	Average A/C ratios	Possible climatic status	Possible climatic period
0-1	1220–960	?–31.5	*Picea*, *Taraxacum*-type, Chenopodiaceae, *Artemisia*	Montane forest–steppe	0.7	Wet	Late MIS3
0-2	960–865	31.5–14.7	Chenopodiaceae, *Artemisia*	Chenopodiaceae desert	0.4	Dry	Early MIS2 (LGM hiatus)
1-1	865–795	14.7–14.5	*Betula*, *Picea*, Chenopodiaceae, *Artemisia*	Coniferous–broad-leaved mixed forest	0.5	Wet	Beginning of Bølling period
1-2	795–655	14.5–13.6	Chenopodiaceae, *Artemisia*	Chenopodiaceae desert	0.3	Dry	?
1-3	655–605	13.6–13.4	*Geranium*, *Aster*-type, Compositae, Chenopodiaceae	Subalpine meadow	0.4	Slight Wet	Older Dryas
1-4	605–535	13.4–12.9	*Artemisia*, Poaceae, *Aster*-type, *Taraxacum*-type	Montane steppe	2.3	More wet	Allerød period
2	535–500	12.9–12.6	Poaceae, Chenopodiaceae, *Artemisia*	Desert steppe	0.5	Slight Dry	Younger Dryas
	500–465	12.6–12.0	Compositae, *Geranium*, *Artemisia*, *Taraxacum*-type	Subalpine meadow	1.0	Slight wet	
	465–455	12.0–11.7	Chenopodiaceae, *Artemisia*	Chenopodiaceae desert	0.1	Very dry	
3	455–400	11.7–10.1	*Artemisia*, Polygonaceae, *Tamarix*	Shrub steppe	2.0	Wet	Preboreal period

The YD cold event has been identified in many parts of the Northern Hemisphere, however particular characteristics of that event vary between regions. For example, in northern Denmark the YD is associated with rising lake levels (Noe-Nygaard and Heiberg, 2001), while in southern Switzerland three phases of lake level change are reported (Magny et al., 2001). Three climatic phases are also reported in the desert-loess transition zone of northern China. There, conditions progressed from being cold and dry, to cool and humid, and then back to cold and dry during the YD (Zhou et al., 1996, 1999; Li et al., 2003). Pollen data from the Yili section indicates that dry conditions prevailed from 12.9 to 11.7 cal kyr BP, which corresponds with the YD period in Greenland and the North Atlantic (Stuiver et al., 1995; Rasmussen et al., 2006) (Fig. 5). Superimposed on this are three distinct phases: during the early YD (12.9–12.6 cal kyr BP) conditions were dry and the region was inhabited by dry desert steppe vegetation characterized by Poaceae and low A/C ratios; during the mid-YD (12.6–12.0 cal kyr BP) moisture levels were slightly elevated as subalpine meadow vegetation dominated by Compositae and *Gerarnium* occurred along with a small rise of A/C ratios; during the late YD (12.0–11.7 cal kyr BP) moisture levels were at their lowest for the deglaciation period and vegetation was dominated by Chenopodiaceae with extremely low A/C ratios (Fig. 5). The three-phase climate fluctuation detected for the Yili Valley is similar to that detected in southern Europe and in the desert–loess transition belt of China.

Following the YD period (11.7–10.1 cal kyr BP) a marked shift in vegetation occurs in the Yili Valley. Shrub steppe communities appear which are dominated by *Artemisia*, Fabaceae and Polygonaceae. Increased moisture levels are indicated by high A/C ratios (2.0 average). This period corresponds to the rapid rise in SSTs in the North Atlantic following the YD (Bard et al., 2000).

The main characteristic of pollen taxa, A/C ratios, inferred vegetation changes and possible climate status are presented in Table 2. Overall, climate changes in the Yili Valley correlate well with those observed in Greenland, the North Atlantic, Europe and Monsoonal Asia (Stuiver et al., 1995; Dykoski et al., 2005), which show instability during the last deglaciation. Some climate variations in the Yili Valley appear to be out of phase with other Northern Hemisphere sites, for example the long dry period from 14.5 to 13.6 cal kyr BP does not appear in the other records mentioned here. This may relate to differences in regional responses to change in oceanic and atmospheric circulation, to differences in local conditions, or to differences in the palaeoenvironmental proxies used. On the other hand, the different sample resolution and age uncertainties compared to the records from Greenland ice core and Hulu cave may also affect the precision of comparison in this study.

This study shows that the onset of the warm Bølling period coincides with increased summer insolation in the Northern Hemisphere, and that moisture changes occurring in western Xinjiang during the last deglaciation are connected with SSTs in the North Atlantic, through the influence of the mid-latitude westerlies. Climate events during the last deglaciation in Yili Valley correlate well with other palaeoclimate records in the Northern Hemisphere, suggesting that those climate changes were forced by the same mechanisms. Changes in the thermohaline circulation of the North Atlantic, and associated change in SSTs, are probably responsible for these millennial to century-scale climate events (Broecker et al., 1985). These changes in the oceans are transmitted by atmospheric circulation to other regions in the world. While this study does not attempt to explain the mechanisms driving climate change in the Yili Valley, it does offer new data to improve the understanding of climate characteristics in central Asia during the last deglaciation.

Acknowledgments

We appreciate the financial support from the National Science Foundation of China (41102113, 41172161), and National Basic Research Program of China (2010CB950204), and the support of colleagues at the Australian Nuclear Science and Technology Organization.

References

Alley, R.B., Meese, D., Shuman, C., Gow, A., Taylor, K., Grootes, P., White, J., Ram, M., Waddington, E., Mayewski, P., 1993. Abrupt increase in Greenland snow accumulation at the end of the Younger Dryas event. Nature 362, 527–529.

Bard, E., Rostek, F., Turon, J., Gendreau, S., 2000. Hydrological impact of Heinrich events in the subtropical northeast Atlantic. Science 289, 1321–1324.

Barker, S., Diz, P., Vautravers, M.J., Pike, J., Knorr, G., Hall, I.R., Broecker, W.S., 2009. Interhemispheric Atlantic seesaw response during the last deglaciation. Nature 457, 1097–1102.

Benson, L., Burdett, J., Lund, S., Kashgarian, M., Mensing, S., 1997. Nearly synchronous climate change in the Northern Hemisphere during the last glacial termination. Nature 388, 263–265.

Berger, A., Loutre, M.F., 1991. Insolation values for the climate of the last 10 million years. Quaternary Science Reviews 10, 297–317.

Blanchon, P., Shaw, J., 1995. Reef drowning during the last deglaciation: evidence for catastrophic sea-level rise and ice-sheet collapse. Geology 23, 4–8.

Blunier, T., Brook, E.J., 2001. Timing of millennial-scale climate change in Antarctica and Greenland during the last glacial period. Science 291, 109.

Boomer, I., Aladin, N., Plotnikov, I., Whatley, R., 2000. The palaeolimnology of the Aral Sea: a review. Quaternary Science Reviews 19, 1259–1278.

Broecker, W., Peteet, D., Rind, D., 1985. Does the ocean–atmosphere system have more than one stable mode of operation? Nature 315, 21–26.

Chen, F.H., Yu, Z.C., Yang, M.L., Ito, E., Wang, S.M., Madsen, B.D., Huang, X.Z., Zhao, Y., Sato, T., Birks, J.H., Boomer, I., Chen, J.H., An, C.B., Wunnemann, B., 2008. Holocene moisture evolution in arid Central Asia and its out-of-phase relationship with Asian monsoon history. Quaternary Science Reviews 27, 351–364.

Clark, P.U., Mix, A.C., 2002. Ice sheets and sea level of the Last Glacial Maximum. Quaternary Science Reviews 21, 1–7.

Cour, P., Zheng, Z., Duzer, D., Calleja, M., Yao, Z., 1999. Vegetational and climatic significance of modern pollen rain in northwestern Tibet. Review of Palaeobotany and Palynology 104, 183–204.

Dansgaard, W., White, J., Johnsen, S., 1989. The abrupt termination of the Younger Dryas climate event. Nature 339, 532–534.

Dansgaard, W., Johnsen, S., Clausen, H., Dahl-Jensen, D., Gundestrup, N., Hammer, C., Hvidberg, C., Steffensen, J., Sveinbjörnsdottir, A., Jouzel, J., 1993. Evidence for general instability of past climate from a 250-kyr ice-core record. Nature 364, 218–220.

Dykoski, C.A., Edwards, R.L., Cheng, H., Yuan, D.X., Cai, Y.J., Zhang, M.L., Lin, Y.S., Qing, J.M., An, Z.S., Revenaugh, J., 2005. A high-resolution, absolute-dated Holocene and deglacial Asian monsoon record from Dongge Cave, China. Earth and Planetary Science Letters 233, 71–86.

Editorial Committee for Vegetation of China, 1980. Vegetation of China. Science Press, Beijing. (in Chinese).

El-Moslimany, A.P., 1990. Ecological significance of common nonarboreal pollen: examples from drylands of the Middle East. Review of Palaeobotany and Palynology 64, 343–350.
Erdtman, G., 1960. The acetolysis method. Svensk Botanisk Tidskrift 54, 561–564.
Gasse, F., Arnold, M., Fontes, J.C., Fort, M., Gibert, E., 1991. A 13000-year climate record from western Tibet. Nature 353, 742–745.
Herzschuh, U., 2006. Palaeo-moisture evolution in monsoonal Central Asia during the last 50,000 years. Quaternary Science Reviews 25, 163–178.
Herzschuh, U., Tarasov, P., Wünnemann, B., Hartmann, K., 2004. Holocene vegetation and climate of the Alashan Plateau, NW China, reconstructed from pollen data. Palaeogeography, Palaeoclimatology, Palaeoecology 211, 1–17.
Herzschuh, U., Kurschner, H., Mischke, S., 2006a. Temperature variability and vertical vegetation belt shifts during the last 50,000 yr in the Qilian Mountains (NE margin of the Tibetan Plateau, China). Quaternary Research 66, 133–146.
Herzschuh, U., Winter, K., Wünnemann, B., Li, S.J., 2006b. A general cooling trend on the Central Tibetan Plateau throughout the Holocene recorded by the Lake Zigetang pollen spectra. Quaternary International 154 (155), 113–121.
Huang, C.X., VanCampo, E., Duobuleimei, F., 1993. A study on pollen in surface soil from the western Xizang. Arid Land Geography 15, 75–84 (in Chinese with English abstract).
Huang, X.Z., Chen, F.H., Fan, Y.X., Yang, M.L., 2009. Dry late-glacial and early Holocene climate in arid Central Asia indicated by lithological and palynological evidence from Bosten Lake, China. Quaternary International 194, 19–27.
Hughen, K.A., Overpeck, J.T., Peterson, L.C., Trumbore, S., 1996. Rapid climate changes in the tropical Atlantic region during the last deglaciation. Nature 380, 51–54.
Imbrie, J., Hays, J.D., Martinson, D.G., Mclntyre, A., Mix, A.C., Morley, J.J., Pisias, N.G., Prell, W.L., Shackleton, N.J., 1984. The orbital theory of Pleistocene climate: support from a revised chronology of the marine δ^{18}O record. In: Berger, A., Imbrie, J., Hays, H., Kukla, G., Saltzman, B. (Eds.), Milankovitch and Climate. Reidal Publish Company, Dordrecht, pp. 269–305.
Karabanov, E., Williams, D., Kuzmin, M., Sideleva, V., Khursevich, G., Prokopenko, A., Solotchina, E., Tkachenko, L., Fedenya, S., Kerber, E., 2004. Ecological collapse of Lake Baikal and Lake Hovsgol ecosystems during the Last Glacial and consequences for aquatic species diversity. Palaeogeography, Palaeoclimatology, Palaeoecology 209, 227–243.
Lehman, S.J., Keigwin, L.D., 1992. Sudden changes in North Atlantic circulation during the last deglaciation. Nature 356, 757–762.
Li, J.F., 1991. Climate in Xinjiang. China Meteorological Press, Beijing.
Li, X.Q., Du, N.Q., 1999. The acid-alkali-free analysis of Quaternary pollen. Acta Botanica Sinica 41, 782–784 (in Chinese with English abstract).
Li, X.Q., Zhou, W.J., An, Z.S., Dodson, J., 2003. The vegetation and monsoon variations at the desert-loess transition belt at Midiwan in northern China for the last 13 ka. The Holocene 13, 779–784.
Li, X.Q., Zhao, K.L., Dodson, J., Zhou, X.Y., 2011. Moisture dynamics in central Asia for the last 15 kyr: new evidence from Yili Valley, Xinjiang, NW China. Quaternary Science Reviews 30, 3457–3466.
Liu, H.Y., Cui, H.T., Pott, R., Speier, M., 1999. The surface pollen of the woodland–steppe ecotone in southeastern Inner Mongolia, China. Review of Palaeobotany and Palynology 105, 237–250.
Liu, Z., Otto-Bliesner, B., He, F., Brady, E., Tomas, R., Clark, P., Carlson, A., Lynch-Stieglitz, J., Curry, W., Brook, E., 2009. Transient simulation of last deglaciation with a new mechanism for Bølling–Allerød warming. Science 325, 310–314.
Lotter, A.F., Ammann, B., Sturm, M., 1992. Rates of change and chronological problems during the late-glacial period. Climate Dynamics 6, 233–239.
Luo, C.X., Zheng, Z., Tarasov, P., Pan, A.D., Huang, K.Y., Beaudouin, C., An, F.Z., 2009. Characteristics of the modern pollen distribution and their relationship to vegetation in the Xinjiang region, northwestern China. Review of Palaeobotany and Palynology 153, 282–295.
Ma, Y.Z., Meng, H.W., Sang, Y.L., Sun, A.Z., Wu, J., Wang, W., 2009. Pollen keys of indentification of Coniferopisa and Compositae classes under light microscopy and their ecological significance. Acta Palaeontologica Sinica 48, 240–253.
Magny, M., Guiot, J., Schoellammer, P., 2001. Quantitative reconstruction of Younger Dryas to Mid-Holocene Palaeoclimates at Le Locle, Swiss Jura, using pollen and lake-level data. Quaternary Research 57, 170–180.
Moore, P.D., Webb, J.A., 1978. An Illustrated Guide to Pollen Analysis. Hodder and Stoughton, London.
Morley, D.W., Leng, M.J., Mackay, A.W., Sloane, H.J., 2005. Late glacial and Holocene environmental change in the Lake Baikal region documented by oxygen isotopes from diatom silica. Global and Planetary Change 46, 221–233.
Murakami, T., Katsuta, N., Yamamoto, K., Takamatsu, N., Takano, M., Oda, T., Matsumoto, G.I., Horiuchi, K., Kawai, T., 2010. A 27-kyr record of environmental change in central Asia inferred from the sediment record of Lake Hovsgol, northwest Mongolia. Journal of Paleolimnology 43, 369–383.
Nakagawa, T., Tarasov, P.E., Kitagawa, H., Yasuda, Y., Gotanda, K., 2006. Seasonally specific responses of the East Asian monsoon to deglacial climate changes. Geology 34, 521–524.
Noe-Nygaard, N., Heiberg, E., 2001. Lake-level changes in the Late Weichselian Lake Tøvelde, Møn, Denmark: induced by changes in climate and base level. Palaeogeography, Palaeoclimatology, Palaeoecology 174, 351–382.
Parizek, B.R., Alley, R.B., 2004. Implications of increased Greenland surface melt under global-warming scenarios: ice-sheet simulations. Quaternary Science Reviews 23, 1013–1027.
Porter, S.C., An, Z.S., 1995. Correlation between climate events in the North Atlantic and China during the last glaciation. Nature 375, 305–308.
Prokopenko, A.A., Williams, D.F., 2004. Deglacial methane emission signals in the carbon isotopic record of Lake Baikal. Earth and Planetary Science Letters 218, 135–147.
Prokopenko, A.A., Kuzmin, M.I., Williams, D.F., Gelety, V.F., Kalmychkov, G.V., Gvozdkov, A.N., Solotchin, P.A., 2005. Basin-wide sedimentation changes and deglacial lake-level rise in the Hovsgol basin, NW Mongolia. Quaternary International 136, 59–69.
Rasmussen, S.O., Andersen, K.O., Svensson, A.M., Steffensen, J.P., Vinther, B.M., Clausen, H.B., Siggaard-Andersen, M.L., Johnsen, S.J., Larsen, Dahl-Jensen, L.B., Bigler, M., Röthlisberger, R., Fischer, H., Goto-Azuma, K., Hansson, M.E., Ruth, U., 2006. A new Greenland ice core chronology for the last glacial termination. Journal of Geophysical Research 111, 1–16.
Reimer, P.J., Baillie, M.G.L., Bard, E., Bayliss, A., Beck, J.W., Blackwell, P.G., Bronk Ramsey, C., Buck, C.E., Burr, G.S., Edwards, R.L., Friedrich, M., Grootes, P.M., Guilderson, T.P., Hajdas, I., Heaton, T.J., Hogg, A.G., Hughen, K.A., Kaiser, K.F., Kromer, B., McCormac, F.G., Manning, S.W., Reimer, R.W., Richards, D.A., Southon, J.R., Talamo, S., Turney, C.S.M., van der Plicht, J., Weyhenmeyer, C.E., 2009. IntCal09 and Marine09 radiocarbon age calibration curves, 0–50,000 years cal BP. Radiocarbon 51, 1111–1150.
Rodrigues, T., Grimalt, J.O., Abrantes, F., Naughton, F., Flores, J., 2010. The last glacial–interglacial transition (LGIT) in the western mid-latitudes of the North Atlantic: abrupt sea surface temperature change and sea level implications. Quaternary Science Reviews 29, 1853–1862.
Ruddiman, F.W., McIntyre, A., 1981. The North Atlantic Ocean during the last deglaciation. Palaeogeography, Palaeoclimatology, Palaeoecology 35, 145–214.
Shang, X., Li, X.Q., An, Z.S., Ji, M., Zhang, H.B., 2009. Modern pollen rain in the Lake Qinghai basin, China. Science in China Series D: Earth Sciences 52, 1510–1519.
Shen, J., Liu, X., Ryo, M., Wang, S., Yang, X., 2005. A high-resolution climatic change since the Late Glacial Age inferred from multi-proxy of sediments in Qinghai Lake. Science in China Series D: Earth Sciences 48, 742–751.
Shi, Y., Yu, G., Liu, X., Li, B., Yao, T., 2001. Reconstruction of the 30–40 ka BP enhanced Indian monsoon climate based on geological records from the Tibetan Plateau. Palaeogeography, Palaeoclimatology, Palaeoecology 169, 69–83.
Sirocko, F., Garbe-Schönberg, D., McIntyre, A., Molfino, B., 1996. Teleconnections between the subtropical monsoons and high-latitude climates during the last deglaciation. Science 272, 526–529.
Sowers, T., Bender, M., 1995. Climate records covering the last deglaciation. Science 269, 210–214.
Stocker, T.F., Wright, D.G., 1991. Rapid transitions of the ocean's deep circulation induced by changes in surface water fluxes. Nature 351, 729–732.
Stuiver, M., Grootes, P.M., Braziunas, T.F., 1995. The GISP2 δ^{18}O climate record of the past 16,500 years and the role of the sun, ocean, and volcanoes. Quaternary Research 44, 341–354.
Sun, X.J., Du, N.Q., Weng, C.Y., Lin, R.F., Wei, K.Q., 1994. Palaeovegetation and palaeoenvironment of Manas Lake, Xinjiang, Northwestern China during the last 14000 years. Quaternary Sciences 3, 239–248 (in Chinese with English abstract).
Swann, G.E.A., Mackay, A.W., Leng, M.J., Demory, F., 2005. Climatic change in Central Asia during MIS 3/2: a case study using biological responses from Lake Baikal. Global and Planetary Change 46, 235–253.
Tao, S.C., An, C.B., Chen, F.H., Tang, L.Y., Wang, Z.L., Lu, Y.B., Li, Z.F., Zhao, J.J., 2010. Pollen-inferred vegetation and environmental changes since 16.7 ka BP at Balikun Lake, Xinjiang. Chin. Chinese Science Bulletin 55, 2449–2457.
Thom, N., 2010. A hydrological model of the Black and Caspian Seas in the late Pleistocene and early-middle Holocene. Quaternary Science Reviews 29, 2989–2995.
Von Grafenstein, U., Erlenkeuser, H., Brauer, A., Jouzel, J., Johnsen, S.J., 1999. A mid-European decadal isotope-climate record from 15,500 to 5000 years B.P. Science 284, 1654–1657.
Wang, F.X., Qian, N.F., Zhang, Y.L., Yang, H.Q., 1997. Pollen Flora of China, Second edition. Science Press, Beijing . (in Chinese).
Wang, Y.J., Cheng, H., Edwards, R.L., An, Z., Wu, J., Shen, C.C., Dorale, J.A., 2001. A high-resolution absolute-dated late Pleistocene monsoon record from Hulu Cave, China. Science 294, 2345–2348.
Weng, C.Y., Sun, X.J., Chen, Y.S., 1993. Numerical characteristics of pollen assemblages of summer samples from the west Kunlun mountains. Acta Botanica Sinica 35, 69–79 (in Chinese with English abstract).
Xi, Y.Z., Ning, J.C., 1994. Study on pollen morphology of plants from dry and semidry area in China. Yushania 11, 119–191 (in Chinese with English abstract).
Xinjiang Expedition Team, Chinese Academy of Sciences, 1978. Vegetation and its Utilization in Xinjiang. Sciences Press, Beijing . (in Chinese).
Xu, Y.Q., Yan, S., Jia, B.Q., Yang, Y.L., 1996. Numerical relationship between the surface spore-pollen and surrounding vegetation on the southern slope of Tianshan Mountains. Arid Land Geography 19, 24–30 (in Chinese with English abstract).
Xu, Q.H., Li, Y.C., Yang, X.L., Zheng, Z.H., 2007. Quantitative relationship between pollen and vegetation in northern China. Science in China Series D: Earth Sciences 50, 582–599.
Yan, S., 1991. The characteristics of Quaternary sporo-pollen assemblage and the vegetation succession in Xinjiang. Arid Land Geography 14, 1–9 (in Chinese with English abstract).
Yan, S., 1993. The discussion on the pollen of Pine family in surface soil in Xinjiang. Arid Land Geography 16, 1–9 (in Chinese with English abstract).
Yan, S., Kong, Z.C., Yang, Z.J., Zhang, Y., Ni, J., 2004. Seeking relationship between vegetation and Picea pollen in surface soil of Xinjiang, northwestern China. Acta Ecologica Sinica 24, 2017–2022 (in Chinese with English abstract).
Yancheva, G., Nowaczyk, N.R., Mingram, J., Dulski, P., Schettler, G., Negendank, J.F.W., Liu, J., Sigman, D.M., Peterson, L.C., Haug, G.H., 2007. Influence of the intertropical convergence zone on the East Asian monsoon. Nature 445, 74–77.
Yu, Z., Eicher, U., 1998. Abrupt climate oscillations during the last deglaciation in central North America. Science 282, 2235–2238.
Yu, Z., Wright Jr., H., 2001. Response of interior North America to abrupt climate oscillations in the North Atlantic region during the last deglaciation. Earth-Science Reviews 52, 333–369.

Yu, G., Xue, B., Liu, J., Chen, X., 2003. LGM lake records from China and an analysis of climate dynamics using a modelling approach. Global and Planetary Change 38, 223–256.

Yuan, D., Cheng, H., Edwards, R.L., Dykoski, C.A., Kelly, M.J., Zhang, M., Qing, J., Lin, Y., Wang, Y., Wu, J., 2004. Timing, duration, and transitions of the last interglacial Asian monsoon. Science 304, 575.

Zhao, Y., Herzschuh, U., 2009. Modern pollen representation of source vegetation in the Qaidam Basin and surrounding mountains, north-eastern Tibetan Plateau. Vegetation History and Archaeobotany 18, 245–260.

Zhou, W.J., Donahue, D., Porter, S., Jull, T., Li, X.Q., Stuiver, M., An, Z.S., Matsumoto, E., Dong, G.R., 1996. Variability of monsoon climate in east Asia at the end of the last glaciation. Quaternary Research 46, 219–229.

Zhou, J., Zhou, W.J., Chen, H.Z., Xue, X.X., Nanson, G., 1999. Evidence for Asian summer monsoon precipitation instability of the Younger Dryas phase. Chinese Science Bulletin 44, 849–852.